Applied Catalysis B: Environmental 231 (2018) 108–114

Contents lists available at ScienceDirect

Applied Catalysis B: Environmental

journal homepage: www.elsevier.com/locate/apcatb

Hydrophilic mesoporous carbon as iron(III)/(II) electron shuttle for visible light enhanced Fenton-like degradation of organic pollutants

Xufang Qian[a], Meng Ren[a], Mengyuan Fang[a], Miao Kan[a], Dongting Yue[a], Zhenfeng Bian[b], Hexing Li[b], Jinping Jia[a], Yixin Zhao[a,*]

[a] School of Environmental Science and Engineering, Shanghai Jiao Tong University, 800 Dongchuan Road, Shanghai 200240, China
[b] The Education Ministry Key Lab of Resource Chemistry and Shanghai Key Laboratory of Rare Earth Functional Materials, Shanghai Normal University, Shanghai 200234, China

ARTICLE INFO

Keywords:
Hydrophilic mesoporous carbon
Iron(III)/(II)
Heterogeneous Fenton
Visible light
Organic pollutants

ABSTRACT

A Fenton-like catalyst comprising of hydrophilic mesoporous carbon (HMC) and ferric ions was found very efficiently in degradation organic pollutants under visible light irradiation in the presence of H_2O_2. HMC with graphene domains and plenty of oxygen containing groups such as carboxyl groups can cooperate with ferric ions to form a visible light active Fe(III)-HMC configuration. Fe(III)-HMC showed obviously enhanced phenol degradation and mineralization efficiencies than that in dark condition. Acidic condition (pH = 3) is not only more superior in phenol degradation but also in iron leaching in comparison with the case at basic conditions (pH = 4.5–7.0) for Fe(III)-HMC. Total organic carbon (TOC) removal efficiency of five typical organic pollutants show that visible light active Fe(III)-HMC catalyst is more efficient than homogeneous Fenton reagents $FeSO_4$/H_2O_2 excluding the temperature effect. Electron spin resonance (ESR) and electrochemical measurements reveal that the presence of active phenoxyl radicals and ligand to metal charge transfer (LMCT) facilitates the cycling of Fe(III)/Fe(II) and inhibit the side reaction via Haber-Weiss reaction. ·OH radicals rather than $\cdot O^{2-}$ and ·OOH were proved as the predominantly active oxidant. The proposed Fe(III)-HMC configuration activated by visible light opens up a new strategy for carbon based materials and iron species in Fenton-like chemistry.

1. Introduction

Pharmaceuticals, personal care products, pesticides and phenolic compounds were widely used in daily life and industry production which were inevitably discharged into surrounding environment and caused series ecological problems [1–3]. Fenton reaction using Fe^{2+}/H_2O_2 as an important advanced oxidation process has been widely served in waste water treatment (Eq. 1). However, the main drawbacks are production of iron residue and undesired side reactions (Eqs. (2)–(3)) [4].

$$Fe^{2+} + H_2O_2 \rightarrow Fe^{3+} + OH^- + OH\cdot \quad k = 6.3 \times 10\, M^{-1} S^{-1} \tag{1}$$

$$OH\cdot + H_2O_2 \rightarrow H_2O + HO_2\cdot \quad k = 3.3 \times 10^7\, M^{-1} S^{-1} \tag{2}$$

$$Fe^{3+} + HO_2\cdot \rightarrow Fe^{2+} + O_2 + H^+ \quad k = 2.7 \times 10^{-3}\, M^{-1} S^{-1} \tag{3}$$

Iron based heterogeneous Fenton-like catalysts such as iron oxides/hydroxides, iron minerals and iron species loaded on solid supports were widely studied due to the low toxicity and wide availability of iron [5–12]. Throughout the heterogeneous Fenton-like mechanism of iron containing solids the efficient catalysis process of H_2O_2 to ·OH by surface Fe^{3+}/Fe^{2+} redox reaction is a decisive step for organic compounds decomposition [13,14]. Normally, the above process is more efficient under acidic condition due to the priority of production of ·OH with higher oxidation potential at low pH value. However, the iron leaching becomes serious in acidic condition due to the reductive dissolution of iron below pH around 4 [15]. Accordingly, ligands or additives were used to confine the ionic iron on the surface of solid catalysts and accelerate the efficient cycle of Fe(III)/Fe(II), thus the Fenton-like (surface Fenton) efficiency enhanced and the ion leaching problem relieved [16–18]. However, owing to the high oxidation potential of ·OH, the small molecular additives were also consumed by the unselective oxidation of ·OH and produced supernumerary degraded products. The Fe^{3+} complexation with 5-sulfosalicylic acid (SSA) on the surface of resin prevented the undesired destruction of ligands by ·OH and also enhanced the utilization efficiency of H_2O_2 [19]. But the above system was greatly influenced by the molecular structure of organic ligand. Accordingly, a stable, efficient and widely available Fenton-like catalytic system is highly desired for organic

* Corresponding author.
E-mail address: Yixin.Zhao@sjtu.edu.cn (Y. Zhao).

https://doi.org/10.1016/j.apcatb.2018.03.016
Received 12 January 2018; Received in revised form 1 March 2018; Accepted 5 March 2018
Available online 06 March 2018
0926-3373/

pollutants treatment.

Carbon-based materials have showed great potential in environmental pollution control due to their excellent chemical and thermal stability, high surface area with controllable surface chemistry and easy metal recovery [20–24]. The activation of H_2O_2 by metal free carbon based materials is highly correlated to their unique surface chemistry [16,25–27]. Based on previous research, carbon based materials contain a variety of active sites such as quinoid and phenolic oxygen containing groups with redox properties [28,29]. Therefore, it is promising to improve and/or assist the Fenton reaction by modifying the surface chemistry of carbon materials.

Here we report the hydrophilic mesoporous carbon with phenoxyl radicals and oxygen containing groups such as carboxyl which cooperated with ferric ions to form the flexible complex structure. Under visible light irradiation, the phenol degradation and mineralization efficiency enhanced obviously in comparison with the case in dark condition. In similarity with homogeneous Fenton reaction, the phenol degradation is more efficient under acidic condition but the iron leaching was lower than that at higher pH values for Fe(III)-HMC/H_2O_2 under visible light irradiation. The electron transfer from hydrophilic MC to Fe(III) resulting Fe(II) was found by the electrochemical measurements. EPR measurements reflected that ·OH radicals produced by the Fenton-like catalysis of H_2O_2 contributed greatly for the organic pollutants degradation.

2. Experimental

2.1. Materials

Poly(propyleneoxide)-block-poly(ethyleneoxide)-block-poly(propyleneoxide) triblock copolymer Pluronic F127(PEO106PPO70PEO106, Mw = 12,600) was purchased from Sigma–Aldrich. Tetraethyl orthosilicate (TEOS), phenol, ethanol, ferric nitrate ($Fe(NO_3)_3{\cdot}9H_2O$), ammonium persulfate (APS), sulfuric acid were obtained from Sinopharm Chemical Reagent Co., Ltd. Sodium hydroxide (NaOH), nitric acid (HNO_3), hydrogen peroxide (H_2O_2, 30%), hydrofluoric acid (HF, ≥40%), formalin solution (HCHO, 37.0–40.0 wt %) were obtained from Shanghai Lingfeng Chemical Reagent Co., Ltd. 5,5-dimethylpyrroline-1-oxide (DMPO) was obtained from Tokyo Chemical Industry Co., Ltd. All chemicals were used without any further purification and all aqueous solutions were prepared by using distilled and deionized water.

2.2. Catalyst preparation

The mesoporous carbon (MC) was synthesized according to the literatures [30]. The hydrophilic MC was obtained by a wet oxidation method. In a typical process, 1.0 g pristine MC was added into 60 mL of mixture solution (1.0 mol/L APS prepared in 2.0 mol/L H_2SO_4). The above suspended solution was stirred and refluxed at 60 °C for 24 h. Then the hydrophilic MC was washed with distilled water and dried in vacuum at 40 °C, named as HMC. To obtain Fe(III)-HMC, 0.4 g of HMC was added into 100 mL of 0.14 mol/L $Fe(NO_3)_3$ and the suspended solution was stirred overnight. Finally, the solids were filtered, washed with distilled water and dried in vacuum at 40 °C, named as Fe(III)-HMC.

2.3. Characterization

X-ray diffraction (XRD) measurements were performed on a Shimadzu XRD-6100 diffractometer using Cu Kα as radiation. The small-angle X-ray scattering (SAXS) patterns were recorded on a small X-ray scattering system (SAXSess mc^2) using Cu Kα radiation. Nitrogen sorption isotherms were measured at 77K with a Micromeritics Tristar 3000 analyzer. The morphology of Fe(III)-HMC was obtained on a scanning electron microscope (SEM, Sirion 200) equipped with energy dispersive spectrometer (EDS, INCA X-Act). Transmission electron microscopy (TEM) were obtained on a JEM 2100F microscope operated at 200 kV. The iron loading on Fe(III)-HMC were measured by inductively coupled plasma-optical emission spectrometry (iCAP™ 7600 ICP-OES). Fourier transform infrared (FT-IR) experiments were conducted on a Tensor 27 FTIR spectrometer (Nicolet 6700), using KBr pellets of the solid samples. Thermogravimetric (TG) analysis was conducted on a Mettler-Toledo TGA/DSC1/1600HT from 30 to 900 °C under Ar atmosphere (20 mL/min) with a ramp rate of 5 °C/min. X-ray photoelectron spectroscopy (XPS) data were obtained on a Kratos Axis

Table 1
Textural properties of MC, HMC and Fe(III)-HMC.

Sample	Fe content (wt%)	S_{BET} (m^2/g)	V_t (cm^3/g)	D (nm)
MC	/	1674	1.00	4.8
HMC	/	1010	0.63	4.5
Fe(III)-HMC	3.5	736	0.48	4.5

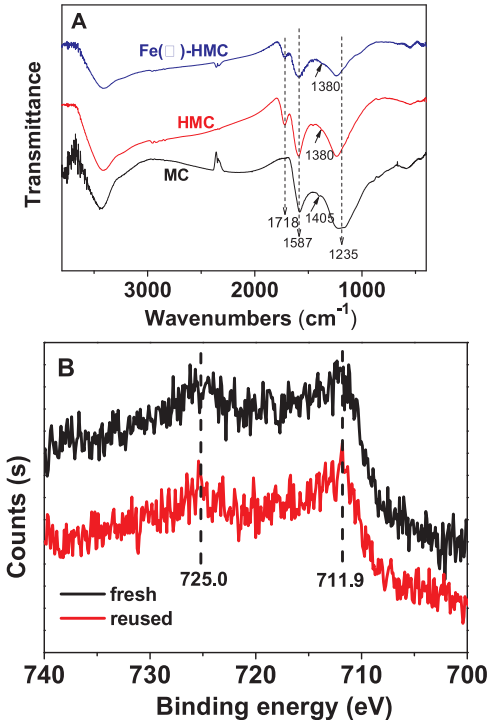

Fig. 1. FTIR spectra of MC, HMC and Fe(III)-HMC (A) and XPS spectrum of Fe $2p_{1/2}$ and $2p_{3/2}$ binding energy for fresh and reused Fe(III)-HMC (B).

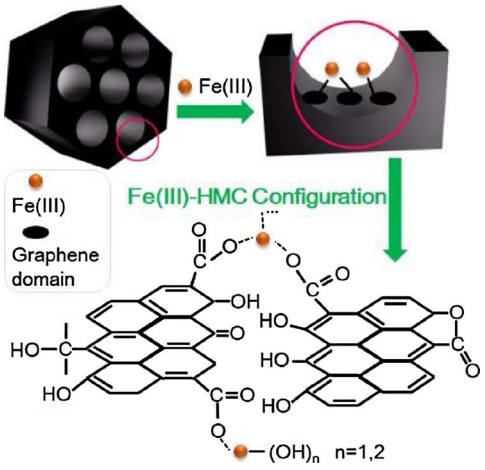

Fig. 2. Schematic illustration of Fe(III)-HMC configuration.

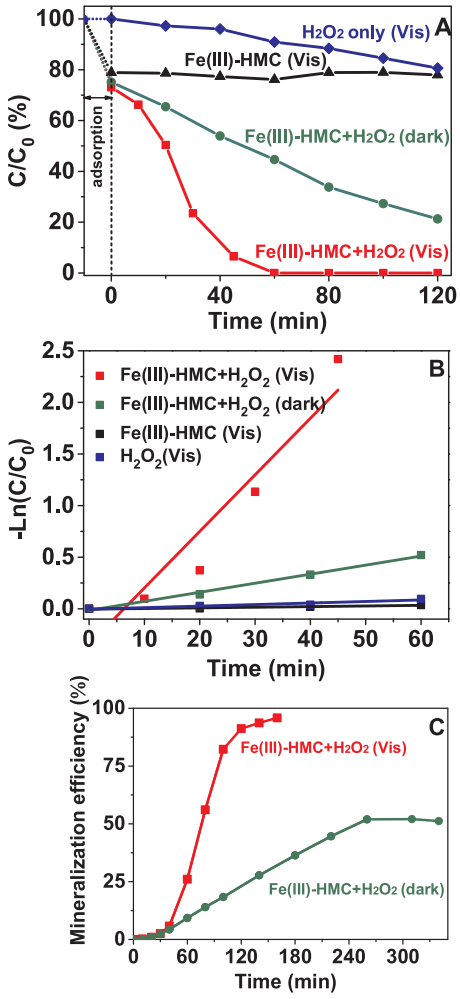

Fig. 3. Phenol degradation curves (A) and the corresponding kinetics (B) at different conditions. Experimental conditions: pH 4.5, 50 mg/L phenol, 0.5 g/L catalyst, 30 mM H_2O_2, 45 °C (in dark); The mineralization efficiency of phenol on Fe(III)-HMC (C). Experimental conditions: pH 4.5, 100 mg/L phenol, 0.5 g/L catalyst, 30 mM H_2O_2, 45 °C (in dark).

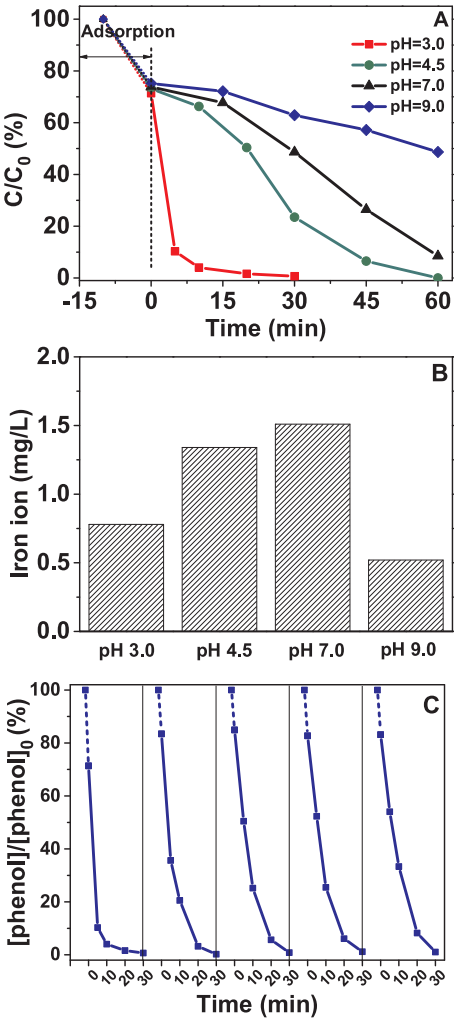

Fig. 4. Fenton-like degradation of phenol on Fe(III)-HMC at different pH values (A) and the corresponding iron ion leaching after 1 h-reaction (B); Reusability of heterogeneous Fenton oxidation efficiency of phenol at pH of 3.0 (C). Experimental conditions: 50 mg/L phenol, 0.5 g/L catalyst dosage, 30 mM H_2O_2, visible light irradiation.

Ultra DLD. Electron paramagnetic resonance (EPR) spectra for radical detection were recorded on a Magnettech MS-5000. Raman spectra were performed on a dispersive Raman Microscope (Senterra R200-L) with an excitation length of 532 nm

2.4. Fenton-like degradation of organic pollutants

Fenton-like oxidation of phenol was carried out in a 40 mL quartz bottle under visible light. Briefly, 15 mg of catalysts and 30 mL of 50 mg/L phenol were added and stirred for 10 min to achieve adsorption equilibrium. Then 90 μL of H_2O_2 was added into the suspension and the bottle was placed in front of a 100 W LED lamp (CEL-LED100) with a 420 nm-cut filter. At a given interval, 0.5 mL aliquots were sampled and filtered through a 0.22 μm filter film for HPLC (SHIMADZU Essentia LC-16) analysis. The mobile phase was a mixture of methanol and water (50: 50, v/v) and the UV detector was operated at 270 nm. The mineralization experiment of phenol was carried out according to our previous work [14]. The concentration of total dissolved irons was measured by 1,10-phenantroline method. Total organic carbon (TOC) data were obtained by a TOC analyzer (multi N/C 3100).

2.5. Electrochemical measurements

Electrochemical measurements were performed using a three-electrode system connected to an electrochemical workstation (CHI 660, CH Instruments). The working electrode was a L-type Glassy-Carbon Electrode (GCE) (diameter: 3 mm) with a PTFE coater, which were polished and cleaned with deionized water. After that, the electrodes were thoroughly rinsed with deionized water. Before being loaded with catalysts, the electrode was also cleaned in an isopropanol solution with sonicating. Ag/AgCl and Pt wire were used as reference and counter electrodes, respectively. Typically, 4 mg of Fe(III)-HMC was dispersed in 1 ml mixture of water and ethanol (4: 1, v/v), and then 80 μl of Nafion solution (5 wt % in water) was added. The suspension

Table 2
TOC removal of recalcitrant organic pollutants.

	Pollutants	Initial conc. (ppm)	TOC removal (%)	
			$FeSO_4$ (dark, 45 °C)	Fe(III)-HMC
1	Phenol	100	50.4	91.8
2	Bisphenol A	100	44.9	67.5
3	Tetracycline	100	35.4	70.6
4	Rhodamine B	100	41.8	83.2
5	Methyl orange	100	58.4	81.0

Experimental condition: pH = 3, catalyst dosage 0.5 g/L ($FeSO_4$ 0.32 mM), 30 mM H_2O_2, visible light irradiation, reaction time 1 h.

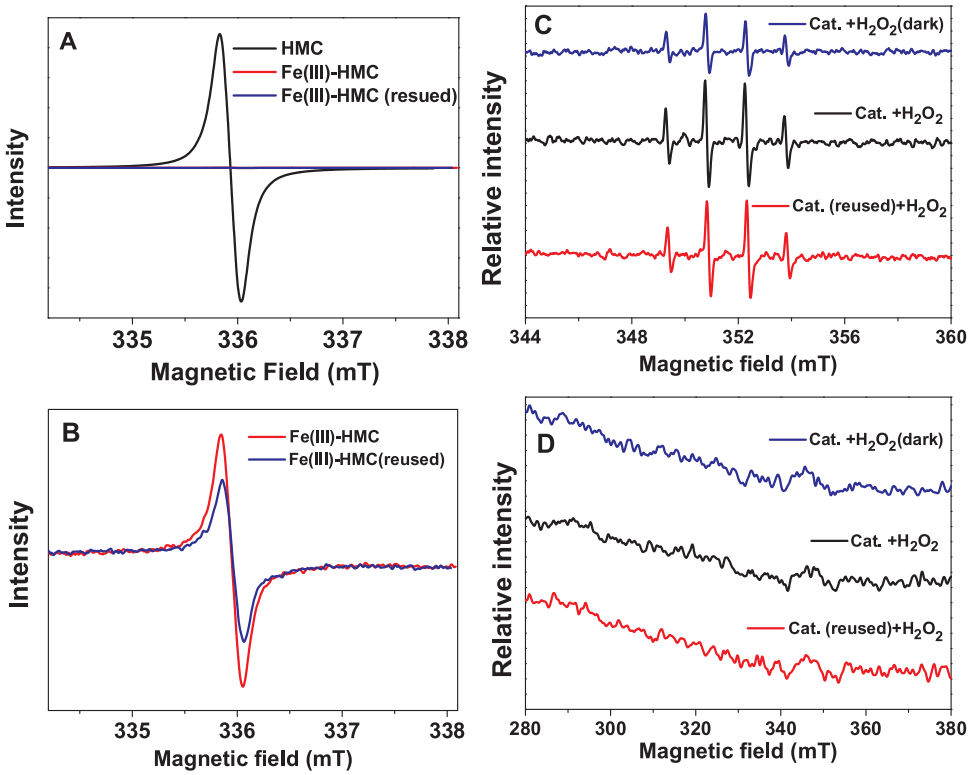

Fig. 5. EPR spectra of 0.01 g HMC, Fe(III)-HMC and reused Fe(III)-HMC (A and B), respectively. Frequency = 100 kHz, center field = 335.9 mT, modulation = 0.2 mT, power = 6.0 mW. DMPO spin-trapping EPR spectra under visible light irradiation in water solutions (C) and in methanol solutions (D).

was immersed in an ultrasonic bath for 30 min to prepare a homogeneous ink. The working electrode was prepared by depositing 5 μl catalyst ink onto GCE.

Cyclic voltammetry (CV) measurements at 100 mV/s were performed for 2 cycles prior to the recording cycle at 50 mV s^{-1} for each sample. Illumination of 100 mW/cm^2 was provided by a tungsten halogen lamp (TeL-150, Ceaulight) as light source. All experiments were performed at ambient temperature (22 ± 2 °C) and electrode potentials were converted to the RHE scale using E(RHE) = E(Ag/AgCl) + 0.197 V + 0.059 × pH.

3. Results and discussion

3.1. Characterizations of Fe(III)-HMC

The wide angle XRD pattern of Fe(III)-HMC remained the same as that of HMC with no obvious diffraction peak observed, revealing that iron loaded on HMC was amorphous (Supporting Information SI, Fig. S1A). The SAXS patterns of HMC and Fe(III)-HMC show two peaks with a strong (100) reflection and a weak (110) reflection assigned to *p6mm* hexagonal symmetry indicating that mesostructure was well preserved after wet oxidation and iron(III) incorporation (SI, Fig. S1B). The TEM images show ordered strip-like and hexagonal arrayed pore structure assigning to the *p6mm* symmetry of Fe(III)-HMC which are in accordance with SAXS data (Fig. S2). The morphology of Fe(III)-HMC is as same as the pristine mesoporous carbon and the corresponding EDS elemental maps demonstrate that C, O and Fe elements are uniformly dispersed in Fe(III)-HMC (Fig. S3).

N_2 sorption isotherms were measured and BET surface areas of MC, HMC and Fe(III)-HMC are 1674, 1010 and 736 m^2/g, respectively (Fig. S4 and Table 1). The V_t values for MC, HMC and Fe(III)-HMC are 1.00, 0.63 and 0.48 cm^3/g, respectively. Both S_{BET} and V_t value decreased successively after wet oxidation and ion adsorption owing to the increased amount of carboxyl groups and Fe(III) coordination in the pore channels [31]. In addition, the pore size distributions are presented in Fig. S4B, with mean values of 4.8, 4.5 and 4.5 nm for MC, HMC and Fe(III)-HMC, respectively. The presence of carboxyl groups after wet oxidation narrowed the pore size. However, the Fe(III) coordination showed weak effect on the pore size.

Raman spectra of HMC and Fe(III)-HMC showed a distinct pair of broad bands at ~ 1590 cm^{-1} (G band) and 1340 cm^{-1} (D band) (Fig. S5). The G band is red-shifted as compared to that of pure graphite (1580 cm^{-1}), suggesting that the graphene sheets in the mesoporous carbons are not fully developed but present as short-range nano-sized graphene sheets [32]. FT-IR spectrum of the MC shows two obvious peaks around 1587 cm^{-1} and 1200 cm^{-1} assigning to the aromatic C═C and C−O stretching of ethers and C═O stretching of carbonyl, and a week peak at 1405 cm^{-1} assigning to C−H bending vibrations indicating that the carbonyl groups (quinone structure) probably conjugated in the defective graphite layer and the small amount of C═C and C−H groups in the surface aromatic structure [31]. An obvious peak appears at 1718 cm^{-1} assigning to the stretching vibration of C═O in undissociated carboxylic acid for HMC and Fe(III)-HMC [33]. Additionally, a peak at ~ 1580 cm^{-1} (overlapping with 1587 cm^{-1}) associate with a very weak peak at 1380 cm^{-1} was found both on HMC and Fe(III)-HMC indicating the conversion of −COOH to $-COO^-$ which proved the Fe(III) chemically interacted with carboxylic group to form electrovalent bond [34]. The C−H groups disappeared on HMC and Fe(III)-HMC indicating the oxidation of C−H into COOH (Fig. 1A). The carboxylic groups (−COOH) concentration was simply calculated to be about 1.5 mmol/g based on the TG curve and thermal analysis (Fig. S6) [35]. The loading amount of Fe(III) ions on HMC is ~0.63 mmol/g (Table 1). XPS spectrum of Fe(III)-HMC shows Fe(III) oxidation state within HMC frameworks in consistent with literature report (Fig. 1B) [19]. Based on the above results, it is concluded that ferric ions are interacting with 1–3 carboxylic groups (O donor ligand) via flexible coordination. A schematic illustration of Fe(III)-HMC configuration was demonstrated that defective graphene layers with surface oxygen containing groups (carboxylic, phenolic and carbonyl) as organic ligands formed the complex structure with ferric ions (Fig. 2).

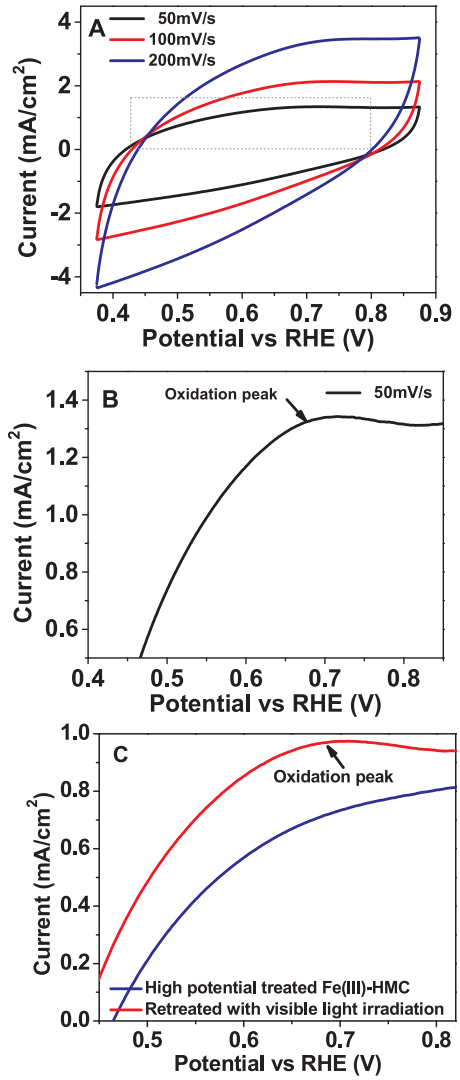

Fig. 6. Cyclic voltammograms of Fe(III)-HMC at different scan rates in 0.1 M Na_2SO_4 solution (pH = 3) (A), the corresponding half CV curve at scan rate of 50 mV/s (B) and the half CV curves of high potential treated Fe(III)-HMC and high potential treated Fe(III)-HMC after visible light irradiation.

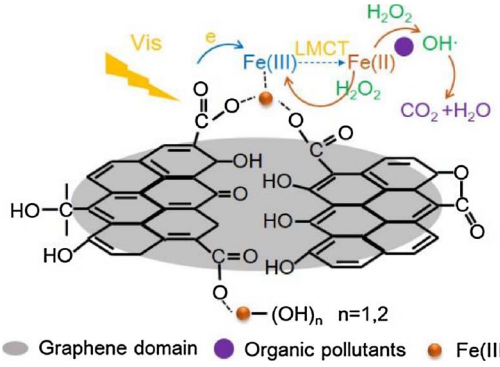

Scheme 1. Visible light induced Fenton-like degradation of organic pollutants on Fe(III)-HMC.

3.2. Visible light induced Fenton-like oxidation of phenol

Phenol was chosen as a model organic pollutant to further evaluate the catalytic activity of Fe(III)-HMC. The initial pH value of reaction suspension was 4.5 without adjustment. The removal efficiency from adsorption on Fe(III)-HMC is about 30% and the adsorption equilibrium was achieved rapidly within 10 min (Fig. S7). To exclude the influence of temperature, the experiment in dark was conducted at 45 °C which was the terminal equilibrium temperature under visible light irradiation (Fig. S8). As shown in Fig. 3A, the degradation efficiency of phenol was achieved 72% within 120 min by heterogeneous Fenton oxidation of Fe(III)-HMC/H_2O_2 in dark, whereas the degradation efficiency greatly improved to be 100% under visible light irradiation within 60 min. In the absence of catalyst, only 20% of degradation efficiency was achieved with H_2O_2 under visible light irradiation and the main intermediate is maleic acid indicating the oxidation potential of H_2O_2 only is low. Additionally, phenol was hardly oxidized by Fe(III)-HMC under visible light irradiation without H_2O_2. The reaction rate constants (k) by first-order kinetic model of phenol oxidation at 45 °C in Fe(III)-HMC/H_2O_2/dark, Fe(III)-HMC/H_2O_2/Vis, Fe(III)-HMC/Vis, H_2O_2/Vis systems were calculated to be 0.0088, 0.055, 0.0015 and 0.0006 min^{-1}, respectively (Fig. 3B). As shown in Fig. 3C, the Fe(III)-HMC/H_2O_2 reached about 91% mineralization efficiency after 120 min under visible light irradiation which is much higher than that (28%) in dark condition. The above results indicate that the degradation of phenol predominantly attributed to the Fenton-like process with H_2O_2, and the degradation efficiency greatly enhanced for Fe(III)-HMC/H_2O_2 under visible light irradiation [36].

3.3. Effect of pH values

For heterogeneous iron based Fenton degradation of organic pollutants, the low pH value (~3) is beneficial for catalyzing the H_2O_2 and producing OH· radicals, however the iron leaching is very serious due to the reduction dissolving of Fe^{2+} [37,38]. The effect of pH values was evaluated on the Fe(III)-HMC/H_2O_2 system under visible light irradiation (Fig. 4A). It is similar with homogeneous Fe^{2+}/H_2O_2 that the phenol oxidation efficiency decreases following the pH increase. The TOF values were calculated to be 0.040, 0.028, 0.014 and 0.0069 min^{-1} for Fe(III)-HMC at initial pH of 3.0, 4.5, 7.0 and 9.0, respectively. It should be noted that the TOF of Fe(III)-HMC/H_2O_2 system under visible light irradiation at pH 7.0 is higher than our previous results [14]. Low pH value is benefit for Fe(III)-HMC/H_2O_2 system under visible light irradiation [4,39]. The iron leaching after 1 h reaction was 0.78, 1.34, 1.51 and 0.52 mg/L for reaction at initial pH of 3.0, 4.5, 7.0 and 9.0, respectively (Fig. 4B). The phenomenon is different with the solid iron based heterogeneous Fenton system, in which low pH value resulted in more serious iron leaching and therefore organic ligands were necessary for confining the reductively dissolved iron on the solid surface [10,17,18]. The concentration of leaching iron ions after 1 h reaction slightly increased from pH 3.0 to 7.0 which was then decreased at pH of 9.0. The results indicate that 1) Fe(III) was very stably anchored on HMC at acidic condition; 2) the soluble iron ion was not the key point for Fenton reaction. High resolution XPS peaks of O 1s for the reused Fe(III)-HMC at initial pH of 3.0, 4.5, 7.0 and 9.0 are shown in Fig. S9 respectively. The O 1s peaks assigning to Fe-O-H (531.8 eV) becomes more obvious after phenol degradation at initial pH of 9.0 for Fe(III)-HMC in comparison with the other case at pH of 3.0–7.0 which should be caused by the hydrolysis of Fe(III) at basic condition. Accordingly, the above results indicate that Fe(III)-HMC/H_2O_2 system is suitable for phenol degradation at acidic condition.

3.4. Catalyst recycling evaluation

To investigate the stability and reusability of Fe(III)-HMC, the reused Fe(III)-HMC were washed with distilled water, dried in vacuum and then reused four times for phenol degradation under visible light irradiation. As observed in Fig. 4C, the removal efficiency of phenol in five cycles all reached to 100% within 30 min, and the degradation rate decreased slightly and kept stable from the second run to the fifth run.

3.5. TOC removal efficiency of organic pollutants

In order to evaluate the mineralization efficiency for different organic pollutants on Fe(III)-HMC, TOC removal efficiency of five typical organic contaminants such as phenol, bisphenol A, tetracycline, rhodamine B and methyl orange were measured after 1h-treatment in Fe(III)-HMC/H_2O_2 under visible light irradiation at pH of 3. For comparison, the TOC removal efficiency in homogeneous Fenton $FeSO_4$/H_2O_2 system was also measured as a control experiment. As listed in Table 2, phenol was achieved the highest TOC removal efficiency (91.8%) in the system of Fe(III)-HMC/H_2O_2 after 1 h reaction. Besides, TOC removal efficiency of Rhodamine B and Methyl orange were achieved higher than 80%. Even for refractory polycyclic aromatic hydrocarbons (PAHs) and antibiotics, the TOC removal efficiency reached 67.5% and 70.6% for Bisphenol A and Tetracycline respectively. This indicated Fe(III)-HMC/H_2O_2 was an efficient and non-selective heterogeneous Fenton catalyst for degradation of organic pollutants. In comparison, the TOC removal efficiencies for five contaminants in homogeneous Fenton system at 45 °C were lower than the case of Fe(III)-HMC/H_2O_2 (Table 2). The corresponding mineralization efficiency of phenol in homogeneous Fenton $FeSO_4/H_2O_2$ system also showed an obvious increase at initial 30 min and subsequent inactive tendency which indicate that the undesired Haber-Weiss reaction inevitably happened owing to the insufficient cycling of Fe^{3+}/Fe^{2+} [4].

3.6. Mechanism

It has been reported that carbonaceous materials with oxygen containing groups possessed persistent free radicals (PFRs) [27,29,40]. EPR results indicate that an obvious singlet signal appears with a *g*-factor of 2.003 (Fig. 5A). The EPR signals with an unchanged *g*-factor of 2.003 was dramatically decreased after corporation with Fe(III) ions indicating that HMC carbonaceous supports possess a large amount of phenoxyl radicals which were quenched by incorporating Fe(III) (Fig. 5B). The signal was decreased for the reused Fe(III)-HMC (Fig. 5B), indicating the possible redox cycle for PFRs radicals [40]. The cyclic voltammogram curves of Fe(III)-HMC show rectangular shapes at different scan rates from 50 mV/s to 200 mV/s and an oxidative peak appears at ~0.7 V indicating the oxidation of Fe(II) in Fe(III)-HMC (Fig. 6A, B) [41]. Based on the above results, Fe(II) was present in Fe(III)-HMC indicating the possibility of single electron transfer from PFRs to Fe(III) producing Fe(II) [40]. The CV curve of Fe(III)-HMC electrode treated with high potential shows negligible oxidation peaks which appears again under consequent visible light irradiation (Fig. 6C). The phenomenon reflects the transformation of Fe(III) to Fe(II) under visible light irradiation.

As shown in Fig. 5C, the generated ·OH radicals were confirmed in dark and visible light condition for the DMPO spin-trapping spectra exhibiting four typical peaks of DMPO-·OH adducts with intensity of 1:2:2:1 for Fe(III)-HMC and reused Fe(III)-HMC, respectively. The other reactive oxygen radicals (ROS) such as DMPO-·O^{2-}, DMPO-·OOH adducts were not present which indicates that ·OH is predominant in Fe(III)-HMC/H_2O_2 system under visible light irradiation and in dark condition, respectively (Fig. 5D).

In Fe(III)-HMC/H_2O_2 Fenton-like system, phenol degradation efficiency was greatly enhanced under visible light irradiation relative to in dark condition (Fig. 3A and C), which should be attributed to the ligand to metal charge transfer (LMCT) of Fe(III) complex in HMC (Scheme 1). Accordingly, we can conclude that the Fe(II) in Fe(III)-HMC originates from the electron transfer between PFRs and Fe(III) and visible light induced LMCT band of Fe(III) complex. In comparison with our previous results, the TOF of phenol oxidation is also very higher in dark condition which attributed to the synergetic carbocatalysis with Fe(III) and production of Fe(II). It is well established that Fe(II) is the most active iron species for catalyzing H_2O_2 to produce ·OH and Fe(III) avoiding undesired decomposition of H_2O_2 via Haber-Weiss reaction. Normally, high generation rate of Fe(II) ions in solid based Fenton-like catalysts resulted in serious iron leaching due to the weak complexation of Fe(II) ions with carboxyl. In the present case, the iron leaching at pH of 3 was low and the phenomenon should be attributed to balance of Fe(III)/Fe(II) cycling during the organic degradation for Fe(III)-HMC/H_2O_2 under visible light irradiation.

4. Conclusions

In summary, we reported a Fenton-like catalyst comprising of hydrophilic mesoporous carbon (HMC) and ferric ions which showed very high efficiency on degradation of organic pollutants under visible light irradiation in the presence of H_2O_2. The electron transfer between PFRs and Fe(III) as well as visible light active ferric complex anchored on HMC facilitated the high generation rate of Fe(II) ions, which contributed to the high TOC removal of five typical recalcitrant organic pollutants. The ·OH radicals were proved to be the predominant oxidants. The iron leaching was low at acidic condition and the recycling test showed high stability of heterogeneous Fenton-like oxidation efficiency. We believe that the novel Fe(III)-HMC configuration activated by visible light provides a new advanced oxidation strategy for organic waste water treatment.

Acknowledgments

This work is supported by National Natural Science Foundation of China (21777097, 21507083, 21777096) and International Joint Laboratory on Resource Chemistry IJLRC-Ministry of Education.

Appendix A. Supplementary data

Supplementary material related to this article can be found, in the online version, at doi:https://doi.org/10.1016/j.apcatb.2018.03.016.

References

[1] J. Su, B. Wei, W. Ou-Yang, F. Huang, Y. Zhao, H. Xu, Y. Zhu, Antibiotic resistome and its association with bacterial communities during sewage sludge composting, Environ. Sci. Technol. 49 (2015) 7356–7363.
[2] Y. Zhu, Y. Zhao, B. Li, C. Huang, S. Zhang, S. Yu, Y. Chen, T. Zhang, M.R. Gillings, J. Su, Continental-scale pollution of estuaries with antibiotic resistance genes, Nat. Microbiol. 2 (2017).
[3] J. Lyu, J. Gao, M. Zhang, Q. Fu, L. Sun, S. Hu, J. Zhong, S. Wang, J. Li, Appl. Catal. B: Environ. 202 (2017) 664–670.
[4] R.L. Siegrist, M. Crimi, T.J. Simpkin, In Situ Chemical Oxidation for Groundwater Remediation, Springer, 2011.
[5] P. Shukla, S. Wang, H. Sun, H. Ang, M. Tade, Adsorption and heterogeneous advanced oxidation of phenolic contaminants using Fe loaded mesoporous SBA-15 and H_2O_2, Chem. Eng. J. 164 (2010) 255–260.
[6] W. Luo, L. Zhu, N. Wang, H. Tang, M. Cao, Y. She, Efficient removal of organic pollutants with magnetic nanoscaled $BiFeO_3$ as a reusable heterogeneous Fenton-like catalyst, Environ. Sci. Technol. 44 (2010) 1786–1791.
[7] C. Sun, C. Chen, W. Ma, J. Zhao, Photodegradation of organic pollutants catalyzed by iron species under visible light irradiation, Phys. Chem. Chem. Phys. 13 (2011) 1957–1969.
[8] H. Jia, J. Zhao, X. Fan, K. Dilimulati, C. Wang, Photodegradation of phenanthrene on cation-modified clays under visible light, Appl. Catal. B: Environ. 123 (2012) 43–51.
[9] X. Yang, X. Xu, J. Xu, Y. Han, Iron oxychloride (FeOCl): an efficient Fenton-like catalyst for producing hydroxyl radicals in degradation of organic contaminants, J. Am. Chem. Soc. 135 (2013) 16058–16061.
[10] X. Hou, X. Huang, F. Jia, Z. Ai, J. Zhao, L. Zhang, Hydroxylamine promoted goethite surface Fenton degradation of organic pollutants, Environ. Sci. Technol. 51 (2017) 5118–5126.
[11] X. Ding, S. Wang, W. Shen, Y. Mu, L. Wang, H. Chen, L. Zhang, Fe@Fe_2O_3 promoted electrochemical mineralization of atrazine via a triazinon ring opening mechanism, Water Res. 112 (2017) 9–18.
[12] Y. Meng, D. Gu, F. Zhang, Y. Shi, L. Cheng, D. Feng, Z. Wu, Z. Chen, Y. Wan, A. Stein, D. Zhao, A family of highly ordered mesoporous polymer resin and carbon structures from organic−organic self-assembly, Chem. Mater. 18 (2006) 4447–4464.
[13] A.A. Nogueira, B.M. Souza, M.W.C. Dezotti, R.A.R. Boaventura, V.J.P. Vilar, Ferrioxalate complexes as strategy to drive a photo-Fenton reaction at mild pH conditions: a case study on levofloxacin oxidation, J. Photochem. Photobiol. A 345 (2017) 109–123.

[14] X. Qian, M. Ren, Y. Zhu, D. Yue, Y. Han, J. Jia, Y. Zhao, Visible light assisted heterogeneous Fenton-like degradation of organic pollutant via alpha-FeOOH/Mesoporous carbon composites, Environ. Sci. Technol. 51 (2017) 3993–4000.
[15] S.S. Chou, C.P. Huang, Y.H. Huang, Heterogeneous and homogeneous catalytic oxidation by supported gamma-FeOOH in a fluidized bed reactor: kinetic approach, Environ. Sci. Technol. 35 (2001) 1247–1251.
[16] J.C. Espinosa, S. Navalon, A. Primo, M. Moral, J.F. Sanz, M. Alvaro, H. Garcia, Graphenes as efficient metal-free Fenton catalysts, Chem. Eur. J. 21 (2015) 11966–11971.
[17] X. Hou, X. Huang, Z. Ai, J. Zhao, L. Zhang, Ascorbic acid/Fe@Fe_2O_3: a highly efficient combined Fenton reagent to remove organic contaminants, J. Hazard. Mater. 310 (2016) 170–178.
[18] X. Huang, X. Hou, F. Jia, F. Song, J. Zhao, L. Zhang, Ascorbate-promoted surface iron cycle for efficient heterogeneous Fenton alachlor degradation with hematite nanocrystals, ACS Appl. Mat. Interfaces 9 (2017) 8751–8758.
[19] H. Ji, W. Song, C. Chen, H. Yuan, W. Ma, J. Zhao, Anchored oxygen-donor coordination to iron for photodegradation of organic pollutants, Environ. Sci. Technol. 41 (2007) 5103–5107.
[20] W. Donphai, T. Kamegawa, M. Chareonpanich, K. Nueangnoraj, H. Nishihara, T. Kyotani, H. Yamashit, Photocatalytic performance of TiO_2-zeolite templated carbon composites in organic contaminant degradation, Phys. Chem. Chem. Phys. 16 (2014) 25004–25007.
[21] W. Wei, C. Yu, Q. Zhao, X. Qian, G. Li, Y. Wan, Synergy effect in photodegradation of contaminants from water using ordered mesoporous carbon-based titania catalyst, Appl. Catal. B: Environ. 146 (2014) 151–161.
[22] X. Qian, M. Ren, D. Yue, Y. Zhu, Y. Han, Z. Bian, Y. Zhao, Mesoporous TiO_2 films coated on carbon foam based on waste polyurethane for enhanced photocatalytic oxidation of VOCs, Appl. Catal. B: Environ. 212 (2017) 1–6.
[23] W. Xu, R. Lan, D. Du, J. Humphreys, M. Walker, Z. Wu, H. Wang, S. Tao, Directly growing hierarchical nickel-copper hydroxide nanowires on carbon fibre cloth for efficient electrooxidation of ammonia, Appl. Catal. B: Environ. 218 (2017) 470–479.
[24] X. Wang, Y. Liang, W. An, J. Hu, Y. Zhu, W. Cui, Removal of chromium (VI) by a self-regenerating and metal free g-C_3N_4/graphene hydrogel system via the synergy of adsorption and photo-catalysis under visible light, Appl. Catal. B: Environ. 219 (2017) 53–62.
[25] S. Navalon, A. Dhakshinamoorthy, M. Alvaro, M. Antonietti, H. Garcia, Active sites on graphene-based materials as metal-free Catalysts, Chem. Soc. Rev. 46 (2017) 4501–4529.
[26] G. Wang, S. Chen, X. Quan, H. Yu, Y. Zhang, Enhanced activation of peroxymonosulfate by nitrogen doped porous carbon for effective removal of organic pollutants, Carbon 115 (2017) 730–739.
[27] Z. Hu, Z. Shen, J.C. Yu, Converting carbohydrates to carbon-based photocatalysts for environmental treatment, Environ. Sci. Technol. 51 (2017) 7076–7083.
[28] L. Kluepfel, M. Keiluweit, M. Kleber, M. Sander, Redox properties of plant biomass-derived black carbon (biochar), Environ. Sci. Technol. 48 (2014) 5601–5611.
[29] Y. Qin, L. Zhang, T. An, hydrothermal carbon-mediated Fenton-like reaction mechanism in the degradation of alachlor: direct electron transfer from hydrothermal carbon to Fe(III), ACS Appl. Mat. Interfaces 9 (2017) 17116–17125.
[30] R.L. Liu, Y.F. Shi, Y. Wan, Y. Meng, F.Q. Zhang, D. Gu, Z.X. Chen, B. Tu, D.Y. Zhao, Triconstituent Co-assembly to ordered mesostructured polymer-silica and carbon-silica nanocomposites and large-pore mesoporous carbons with high surface areas, J. Am. Chem. Soc. 128 (2006) 11652–11662.
[31] Z. Wu, P.A. Webley, D. Zhao, Comprehensive study of Pore evolution, mesostructural stability, and simultaneous surface functionalization of ordered mesoporous carbon (FDU-15) by wet oxidation as a promising adsorbent, Langmuir 26 (2010) 10277–10286.
[32] Z. Wu, Y. Lv, Y. Xia, P.A. Webley, D. Zhao, Ordered mesoporous platinum@graphitic carbon embedded nanophase as a highly active, stable, and methanol-tolerant oxygen reduction electrocatalyst, J. Am. Chem. Soc. 134 (2012) 2236–2245.
[33] C. Moreno-Castilla, M.V. Lopez-Ramon, F. Carrasco-Marin, Changes in surface chemistry of activated carbons by wet oxidation, Carbon 38 (2000) 1995–2001.
[34] H. Kodama, M. Schnitzer, Effect of fulvic acid on the crystallization of Fe(III) oxides, Geoderma 19 (1977) 279–291.
[35] Y. Otake, R.G. Jenkins, Characterization of oxygen-containing surface complexes created on a microporous carbon by air and nitric acid treatment, Carbon 31 (1993) 109–121.
[36] W. Shi, D. Du, B. Shen, C. Cui, L. Lu, L. Wang, J. Zhang, Synthesis of yolk shell structured Fe_3O_4@void@CdS nanoparticles: a general and effective structure design for photo-Fenton reaction, ACS Appl. Mater. Interfaces 8 (2016) 20831–20838.
[37] P. Bautista, A.F. Mohedano, M.A. Gilarranz, J.A. Casas, J.J. Rodriguez, Application of Fenton oxidation to cosmetic wastewaters treatment, J. Hazard. Mater. 143 (2007) 128–134.
[38] M. Hartmann, S. Kullmann, H. Keller, Wastewater treatment with heterogeneous Fenton-type catalysts based on porous materials, J. Mater. Chem. 20 (2010) 9002–9017.
[39] L. Clarizia, D. Russo, I. Di Somma, R. Marotta, R. Andreozzi, Homogeneous photo-Fenton processes at near neutral pH: a review, Appl. Catal. B: Environ. 209 (2017) 358–371.
[40] G. Fang, J. Gao, C. Liu, D.D. Dionysiou, Y. Wang, D. Zhou, Key role of persistent free radicals in hydrogen peroxide activation by biochar: implications to organic contaminant degradation, Environ. Sci. Technol. 48 (2014) 1902–1910.
[41] M. Kim, J. Kim, Synergistic interaction between pseudocapacitive Fe_3O_4 nanoparticles and highly porous silicon carbide for high-performance electrodes as electrochemical supercapacitors, Nanotechnology 28 (2017).